Introduction to Axion Dark Matter: Theory and Experimental Searches

PHYS 363: Particle Physics
Final Paper

Geoffrey Zheng
University of Chicago

June 6, 2021

Abstract

This final paper presents a comprehensive overview of axion dark matter in the context of particle physics. Axions are a leading candidate for dark matter, and also potentially solve the strong CP fine-tuning problem in the Standard Model, which can further our understanding of the matter-antimatter asymmetry in our Universe. The outline of this paper is as follows. In the first section, I elaborate on the particle physics motivations for the existence of axions. This includes an extensive discussion of CP violation in the Standard Model, which then leads to an introduction to the strong CP problem. Separately, I also introduce the basic principles of dark matter. In the second section, I discuss why axions are a suitable candidate for solving the strong CP problem and for being dark matter. This is followed by an introduction to theoretical properties of axions and how they couple to Standard Model particles. Finally, in the third section, I examine current experimental methods for directly detecting axions in Nature. This includes an overview of current axion detection experiments such as ADMX and HAYSTAC, as well as an introduction to a new and promising method for axion detection that involves techniques from atomic, molecular, and optical (AMO) physics.

1 Particle Physics Motivations for Axions

The Standard Model of Particle Physics (SM) is a highly successful SU(3)×SU(2)×U(1) gauge quantum field theory (QFT) that describes three of the four known fundamental interactions in Nature: electromagnetic, strong, and weak. In addition, it classifies all known elementary particles into several categories. These include the quarks and leptons that make up all known matter; the gauge (vector) bosons that act as the force carriers for the fundamental interactions; and the Higgs (scalar) boson that gives mass to all particles [1, 2].

Largely formulated by the mid-1970s, the SM successfully explains a wide range of phenomena in our Universe. However, there remain many outstanding questions in elementary particle physics and cosmology that cannot be explained by the SM, which are largely grouped together as "Beyond the Standard Model Physics" (BSM). Here, I briefly introduce several of the most well-known BSM physics problems. First and foremost, the SM in its current form is not fully compatible with the General Theory of Relativity (GR) at all energy scales, meaning that gravity is the only known fundamental interaction not incorporated in the SM. Many efforts towards developing a theory of quantum gravity are focused on uniting the SM and GR into a singular "Theory of Everything" that describes all four known fundamental interactions as manifestations of a single unified force [1, 3]. Second, rapid advances in observational cosmology in the past few decades provided convincing evidence that dark matter (DM) and dark energy (DE) exist in our Universe. This so-called "dark sector" comprises nearly 95% of the matter-energy content of our Universe, with the remaining 5% coming from the baryonic matter that is already classified in the SM. Since the SM does not supply any fundamental particles or energies that would be good candidates for dark matter or dark energy, the fundamental nature of DM and DE still remains unknown [1–4]. Other BSM phenomena of interest include: the observed matter-antimatter asymmetry in our Universe, which is known as the baryogenesis problem [5]; the fine-tuning in the strengths of the fundamental interactions, which is known as the hierarchy problem [6]; and the fine-tuning in the CP symmetry of the strong interaction, which is known as the strong CP problem [7]. The two BSM phenomena that I will discuss in further detail in the following sections because they pertain to axions are the strong CP problem and the nature of dark matter. To motivate the strong CP problem, I start by discussing parity (P) and charge conjugation-parity (CP) violation in the Standard Model.

1.1 Parity (P) and Charge-Parity (CP) Symmetry Violation

Symmetries play a fundamental role in quantum field theory and elementary particle physics. In the context of physics, a symmetry of a physical system refers to an operation that one can perform on the system to leave it invariant, so that the physics of the system remains the same after the operation is performed. One of the most fundamental results in theoretical physics is Noether's Theorem, which states that every symmetry of a physical system corresponds to a conservation law for that system, and vice versa. For example, if a system has continuous rotational symmetry, then angular momentum is conserved in that system.

Discrete symmetries such as charge conjugation, parity, and time reversal (collectively known as CPT) are of particular interest to particle physicists [1, 8, 9]. Here, I introduce the definitions of each of these symmetries as follows. Charge conjugation (C) symmetry refers to the operation of changing the sign of all of the internal quantum numbers of the particles in a system, i.e. the electric charge, baryon number, lepton number, etc., while not changing the mass, energy, momentum, and

spin. Essentially, this converts all particles in the system to their corresponding antiparticles:

$$C\left|\psi(\vec{x},t)\right\rangle = \left|\bar{\psi}(\vec{x},t)\right\rangle. \tag{1}$$

Parity (P) symmetry refers to the operation of changing the sign of all the spatial coordinates of the particles in a system. This is effectively the same as observing the system of interest in a mirror, or changing the reference frame of a system from right-handed to left-handed:

$$P\left|\psi(\vec{x},t)\right\rangle = \left|\psi(-\vec{x},t)\right\rangle. \tag{2}$$

Time reversal (T) symmetry refers to the operation of reversing the direction of time flow in a physical system, i.e. changing the clocks from running forwards to running backwards:

$$T\left|\psi(\vec{x},t)\right\rangle = \left|\psi(\vec{x},-t)\right\rangle. \tag{3}$$

Up until 1956, physicists believed that the C, P, and T discrete symmetries were all separately conserved in any physical system [10]. However, in 1956, C.N. Yang and T.D. Lee proposed that parity symmetry may be violated in the Weak interaction [11]. To test their proposal, Madame C.S. Wu carried out a nuclear physics experiment that involved the detection of electrons emitted from the β-decay of extremely cold Cobalt-60 nuclei placed in an external magnetic field:

$$^{60}\mathrm{Co} \rightarrow ^{60}\mathrm{Ni} + \mathrm{e}^{-} + \bar{\nu}_e. \tag{4}$$

This process is mediated by the Weak interaction. Wu observed that the electrons were always preferentially emitted with a polar angle opposite to the direction of the external B-field [2, 12]. If parity were conserved in such an interaction, then the electrons should have been emitted isotropically, so Wu's experiment proved that parity was not conserved in the Weak interaction.

After the results of the Wu experiment were published, physicists accepted that parity itself was no longer a fundamental symmetry of Nature. However, they believed that combinations of the discrete symmetries still constituted exact symmetries of Nature. In particular, in 1957, Lev Landau proposed that charge conjugation-parity (CP) symmetry should still be conserved [13]. The combined CP symmetry means that when all particles in a system are changed to their corresponding antiparticles, and their spatial coordinates are inverted, then the physics of the system remains invariant (see Fig. 1 for a visual depiction). After the proposal of CP symmetry conservation, experimentalists quickly set out to test whether CP symmetry indeed remained a good symmetry of Nature or not.

It turns out that neutral K mesons (kaons), denoted by $K^0 = d\bar{s}$, serve as the perfect experimental testbed for CP violation [1, 2, 8]. The reason is that, through a four-vertex 'box diagram' process mediated by the Weak interaction, they can mix with their antiparticle $\overline{K^0}$: $K^0 \longleftrightarrow \overline{K^0}$. Furthermore, neutral kaons are the lightest mesons that contain strange quarks, so they only decay through the Weak interaction. Due to kinematic constraints, K^0 and $\overline{K^0}$ typically decay into either 2 or 3 pions. Now, neutral kaons are pseudoscalars, so under the action of CP, their flavor eigenstate obeys:

$$CP\left|K^0\right\rangle = -\left|\overline{K^0}\right\rangle; \qquad CP\left|\overline{K^0}\right\rangle = -\left|K^0\right\rangle. \tag{5}$$

Therefore, using simple linear algebra, it can be seen that the normalized kaon eigenstates of CP are:

$$\left|K_1\right\rangle = \frac{1}{\sqrt{2}}\left(\left|K^0\right\rangle - \left|\overline{K^0}\right\rangle\right); \qquad \left|K_2\right\rangle = \frac{1}{\sqrt{2}}\left(\left|K^0\right\rangle + \left|\overline{K^0}\right\rangle\right), \tag{6}$$

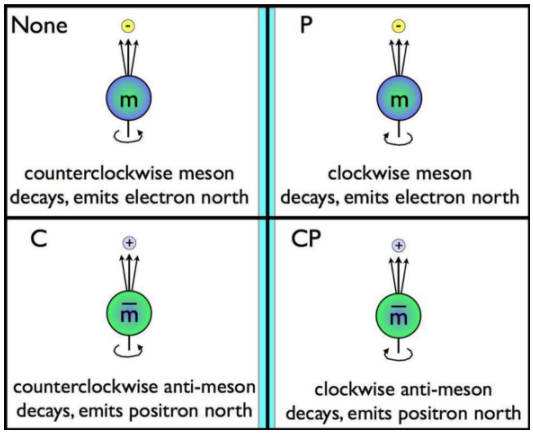

Figure 1: This simple cartoon diagram shows how C, P, and CP symmetries act on the initial system of a spin-up meson that decays and emits an electron in the same direction as the spin. Figure taken from E. Spiegel, *Beyond the Galaxy*.

where it follows that:

$$CP\,|K_1\rangle = |K_1\rangle\,; \qquad CP\,|K_2\rangle = -\,|K_2\rangle\,. \tag{7}$$

This means that, if CP symmetry is conserved in the Weak interaction, then the $|K_1\rangle$ eigenstate can only decay into into a state with CP eigenvalue $= +1$, and $|K_2\rangle$ eigenstate can only decay into a state with CP eigenvalue -1. It turns out that a two-pion system has CP $= +1$ and a three-pion system has CP $= -1$, so it follows that $|K_1\rangle$ should only decay into 2π and $|K_2\rangle$ should only decay into 3π. Finally, because the kaon to 2π decay releases more energy, its decay rate is much faster than the kaon to 3π decay. So in the regime where CP symmetry is conserved in the Weak interaction, we can treat $|K_1\rangle \equiv |K_S\rangle$ to be the short-lived kaon state and $|K_2\rangle \equiv |K_L\rangle$ to be the long-lived kaon state.

This mechanism provided a simple way for particle physicists to test CP violation. In 1964, Val Fitch and James Cronin conducted the following neutral kaon experiment. They produced a beam of K^0 and counted the number of 2π decays observed at the end of the beam line, 57 feet away from the source. This distance is long enough that there should have only been long-lived kaon decays (3π) at that point. However, Fitch and Cronin reported that they counted 45 2π decays out of approximately 22700 total decays [14]. This observation provided irrefutable evidence that CP symmetry was violated in the Weak interaction, since it meant that the long-lived kaon state is not actually a perfect eigenstate of CP:

$$|K_L\rangle = \frac{1}{\sqrt{1+|\epsilon|^2}}(|K_2\rangle + \epsilon\,|K\rangle_1), \tag{8}$$

where $\epsilon \approx 2.24 \times 10^{-3}$ quantifies the deviance of the Weak interaction from CP invariance. Now, although Fitch and Cronin had demonstrated CP violation in the Weak interaction, the effect was minuscule. Physicists wanted to test CP violation in other Weak-mediated decays where the effect might be larger, and in 1981, Carter and Sanda noted that CP violation in neutral B meson decay should be a relatively large effect, albeit in much rarer decays [15]. By the early 2000s, the BaBar (at Stanford Linear Accelerator) and Belle (at KEK) experiments had measured CP violation via the following B meson decays:

$$B^0 \to K^+ + \pi^- \tag{9}$$

$$\overline{B^0} \to K^- + \pi^+, \tag{10}$$

where it was found that the first process was 13% more likely to occur than the second one, even though they transform into each other under CP [16].

Once CP violation in the Weak interaction was established as a fact of Nature, physicists needed to incorporate it into the SM. Since CP violation has only ever been observed in the quark sector of Weak interactions, the CP-violating term turns out to be the complex phase in the Cabibbo-Kobayashi-Maskawa (CKM) matrix [1, 8] that relates the quark flavor eigenstates (unprimed) to the quark weak eigenstates (primed):

$$\begin{pmatrix} d' \\ s' \\ b' \end{pmatrix} = \begin{pmatrix} V_{ud} & V_{us} & V_{ub} \\ V_{cd} & V_{cs} & V_{cb} \\ V_{td} & V_{ts} & V_{tb} \end{pmatrix} \begin{pmatrix} d \\ s \\ b \end{pmatrix} \tag{11}$$

$$V = \begin{pmatrix} c_{12}c_{13} & s_{12}c_{13} & s_{13}e^{-i\delta} \\ -s_{12}c_{23} - c_{12}s_{23}s_{13}e^{i\delta} & c_{12}c_{23} - s_{12}s_{23}s_{13}e^{i\delta} & s_{23}c_{13} \\ s_{12}c_{23} - c_{12}s_{23}s_{13}e^{i\delta} & -c_{12}c_{23} - s_{12}s_{23}s_{13}e^{i\delta} & c_{23}c_{13} \end{pmatrix}, \tag{12}$$

where in the second equation, the canonical form of the CKM matrix is given; $c_{ij} \equiv \cos\theta_{ij}$ and $s_{ij} \equiv \sin\theta_{ij}$ where θ_{ij} are the generalized Cabibbo angles that allow quark mixing between generations, and δ is the complex phase. The mechanism by which the δ term contributes to CP violation can be seen as follows. Consider two particle physics processes:

$$A \to B; \qquad \tilde{A} \to \tilde{B}, \tag{13}$$

where the second process is the first process after CP has been applied. Denote $\mathscr{M}$ and $\tilde{\mathscr{M}}$ to be the matrix amplitude of the first and second processes, respectively. Then, since the second process is charge-conjugated with respect to the first, its matrix amplitude will derive from the complex conjugate of the CKM matrix. So, since $\mathscr{M}$ is a complex number, it is true that:

$$\mathscr{M} = |\mathscr{M}|e^{i\theta}e^{i\delta}; \qquad \tilde{\mathscr{M}} = |\mathscr{M}|e^{i\theta}e^{-i\delta}, \tag{14}$$

where the two processes share the same ordinary phase θ but the CKM phase δ flips sign due to charge conjugation. Now, all physically measurable processes in particle physics, such as scattering or decay rates, depend on $|\mathscr{M}|^2$. If CP symmetry were not violated, then $|\mathscr{M}|^2 = |\tilde{\mathscr{M}}|^2$. However, consider the case where the $A \to B$ process can proceed via at least two distinct mechanisms (the B meson decay that BaBar and Belle measured is an example of this). For the case of two mechanisms, the total matrix amplitude of the process is:

$$\mathscr{M} = |\mathscr{M}_1|e^{i\theta_1}e^{i\delta_1} + |\mathscr{M}_2|e^{i\theta_2}e^{i\delta_2}; \tag{15}$$

and for the CP-applied process:

$$\tilde{\mathscr{M}} = |\mathscr{M}_1|e^{i\theta_1}e^{-i\delta_1} + |\mathscr{M}_2|e^{i\theta_2}e^{-i\delta_2}, \tag{16}$$

where $\theta_1 \neq \theta_2$ and $\delta_1 \neq \delta_2$ because the mechanisms are distinct. Then, it follows from basic manipulation of complex numbers that:

$$|\mathscr{M}|^2 - |\tilde{\mathscr{M}}|^2 = -4|\mathscr{M}_1||\mathscr{M}_2|\sin(\theta_1 - \theta_2)\sin(\delta_1 - \delta_2) \neq 0. \tag{17}$$

Since the difference between $|\mathscr{M}|^2$ and $|\tilde{\mathscr{M}}|^2$ is nonzero due to $\delta_1 \neq \delta_2$, there is a measurable physical difference between the two processes, and CP symmetry is not conserved.

The fact that CP symmetry is violated in the Weak interaction has profound implications for the nature of our Universe. In particular, CP violation provides a mechanism in the early Universe for allowing more matter than antimatter to be produced, leading to the observed matter-antimatter asymmetry today [1, 2, 5]. Astronomers have determined that there cannot be any large-scale cosmological structures comprised of antimatter in our observable Universe, because if there were, the photons produced by electron-positron annihilation at the boundary between the matter and antimatter sections of the Universe should have been observed by us. Quantitatively, the matter-antimatter symmetry can be characterized by the following ratio that is deduced from Big Bang Nucleosynthesis calculations [2]:

$$\frac{n_B - n_{\overline{B}}}{n_\gamma} \sim 10^{-9}, \tag{18}$$

where n_B is the number density of baryons, $n_{\bar{B}}$ is the number density of antibaryons, and n_γ is the number density of photons. What this means is that for every 10^9 antibaryons in the early Universe, there were $10^9 + 1$ baryons, which annihilated to give 10^9 photons and 1 leftover baryon today. But on the other hand, if CP symmetry were not violated in Nature, then theoretical calculations of n_B and $n_{\overline{B}}$ would give:

$$n_B = n_{\overline{B}} \sim 10^{-18} n_\gamma, \tag{19}$$

i.e. there should be equal numbers of baryons and antibaryons in the Universe. Therefore, CP violation provides a crucial mechanism for realizing matter-antimatter asymmetry. However, CP violation has only ever been observed in the Weak interactions of quarks, and this does not provide enough possible processes to account for all of the entire matter-antimatter asymmetry. Therefore, it is still an open question as to what other particle physics processes are CP-violating and so can contribute to the matter-antimatter asymmetry. One possible candidate is the Weak interactions in the leptons, especially after the discovery of neutrino oscillations which implied that neutrinos have mass [17,18]. This led to the development of a leptonic analog to the CKM matrix called the PMNS matrix that provides an analogous mechanism for CP violation in the leptons [1, 2]. However, no CP-violating process in Weak leptonic processes has ever been observed to date. The other possible candidate, which I will discuss in Section 1.2, is CP violation in the Strong interactions.

1.2 The Strong CP Problem

The strong CP problem is a fine-tuning problem in the Standard Model that pertains to the lack of observed CP symmetry violation in the Strong interaction [7, 19–22]. As I discussed in Section 1.1, CP violation is a fundamental fact of Nature that is incorporated into the Weak interaction via the complex phases of the CKM and PMNS matrices. As it turns out though, CP violation is also allowed in quantum chromodynamics (QCD, the theory of the strong interaction). Therefore, since CP violation has only ever been observed in the Weak interactions of quarks, physicists consider it particularly unusual that CP violation has never been observed in the strong interaction. Furthermore, as I mentioned in Section 1.1, CP violation is directly related to the observed matter-antimatter asymmetry in our Universe. Since CP violation in the Weak interactions of quarks is not enough to account for the total observed asymmetry today, it is of particular interest to physicists to understand the other mechanisms in the Standard Model that allow for CP violation, and why they have not been observed yet.

The mechanism for CP violation in the strong interaction is much less obvious than the case of the Weak interaction. To understand how QCD allows for CP violation, recall the QCD Lagrangian that was introduced in our course [1, 19, 22] (in units where $4\pi = \hbar = c = 1$):

$$\mathcal{L}_{\text{QCD}} = -\frac{1}{4} G^a_{\mu\nu} G^{\mu\nu}_a + \sum_f \overline{\psi_f}(i\gamma^\mu D_\mu - m_f)\psi_f; \tag{20}$$

$$G^a_{\mu\nu} \equiv \partial_\mu A^a_\nu - \partial_\nu A^a_\mu - g_s(\vec{A}_\mu \times \vec{A}_\nu)^a; \qquad D_\mu \equiv \partial_\mu + \frac{ig_s}{2}\vec{\lambda}\cdot\vec{A}_\mu; \tag{21}$$

$$(\vec{A}_\mu \times \vec{A}_\nu)^a_i \equiv \left(\sum_{j,k=1}^{8} f_{ijk} \vec{A}_{\mu,j} \vec{A}_{\nu,k} \right)^a. \tag{22}$$

Here, the QCD Lagrangian consists of a sum over all quark flavors f; ψ_f denotes the "3-vector" of spinors corresponding to the 3 colors of each quark flavor; and m_f is the associated mass of each quark flavor. $G^a_{\mu\nu}$ is the gluon field strength tensor in QCD that is analogous to the EM field strength tensor $F_{\mu\nu}$ in QED (a is the additional index needed to index the color degree of freedom). $\vec{A}$ is the gluon gauge field, which is an 8-component vector of four-vectors. g_s is the strong coupling constant that is analogous to electric charge in QED. D_μ is the covariant derivative that is defined in terms of the gluon field and the 8-component vector of Gell-Mann matrices $\vec{\lambda}$. And finally, f_{ijk} are the structure constants of the SU(3) group that are used in QCD.

Note that in the limit of $m_f \ll \Lambda_{\text{QCD}}$ where $\Lambda_{\text{QCD}} \sim 1$ GeV is the QCD phase transition temperature, the m_f term can be ignored in the QCD Lagrangian (eq. 20). Only two flavors of quarks, up and down, satisfy this condition. So by inspection of the form of the Lagrangian in the $m_f \to 0$ limit, it is expected that the strong interactions should be approximately invariant under the global $U(2)_V \times U(2)_A$ symmetry, where $U(2)$ corresponds to the up and down quark that can be approximated as massless [7]. Here, the V indicates the vector component and A indicates the axial component. Experimentally, it is known that $U(2)_V$ corresponds to baryon number conservation and is thus a good symmetry of Nature [19]. However, it turns out that $U(2)_A = SU(2)_A \times U(1)_A$ is not a good symmetry of Nature, with only $SU(2)_A$ being the actual good symmetry. Weinberg called this the $U(1)_A$ problem and suggested that there was no $U(1)_A$ symmetry in the strong interactions [23]. 't Hooft confirmed that QCD did not have $U(1)_A$ symmetry because of the more complicated nature of the QCD vacuum; the exact details of why this is the case go beyond the QFT scope of this course [24]. To resolve this problem, he introduced an anomalous symmetry-breaking of $U(1)_A$ that effectively added the following term to the QCD Lagrangian [7]:

$$\mathcal{L}_\theta = \theta \frac{g_s^2}{32\pi^2} G^{\mu\nu}_a \tilde{G}_{a\mu\nu}. \tag{23}$$

Here, $G^{\mu\nu}_a$ is the same gluon field strength tensor as in eq. (20), and $\tilde{G}_{a\mu\nu} = \frac{1}{2}\epsilon_{\mu\nu\alpha\beta} G^{\alpha\beta}_a$ is the dual of $G^{\mu\nu}_a$; here, $\epsilon_{\mu\nu\alpha\beta}$ is the type (0,4) fully antisymmetric Levi-Civita tensor. It is precisely the θ term in the Lagrangian that allows for CP violation. To understand why without delving into the gory QFT details, it suffices to understand the following intuitive analogy.

It is apparent from the form of the θ "CP-violating" term (eq. 23) that θ affects the properties of the gluon fields. Therefore, it is expected to physically manifest itself in any process or bound system where gluons interact with quarks or with each other. The nucleons (i.e. protons and neutrons) are a prime example of such a system. It turns out that neutron electric dipole moment (nEDM)

measurements are one of the most sensitive tests to CP violation in the strong interaction. Since neutrons consist of 1 up quark and 2 down quarks bound together by gluons, we can qualitatively estimate that the nEDM should characteristically be of the following form:

$$|\vec{d}_N| \sim \theta \cdot e \cdot 10^{-13}\,\text{cm}, \tag{24}$$

where 10^{-13} cm is simply the mean square radius of the neutron. In other words, because θ affects the gluons, it should show up as a simple multiplicative factor in the nEDM formula; there is simply no reason for it to have any other type of complicated dependence on θ. Now, it is a fact that the direction of $\vec{d}_n$ will either be parallel or anti-parallel to the neutron's spin $\vec{s}_n$ [20]; without loss of generality, we can choose it to be parallel. Under CP transformation, $\vec{s}_n$ will not change sign because it is an axial vector, whereas $\vec{d}_n$ will change sign because it is a regular vector. So if $\vec{d}_n \propto \vec{s}_n$ in the original frame, then in the CP-transformed frame, $\vec{d}_n \propto -\vec{s}_n$. But, since the neutron is a neutral spin-1/2 particle, it must transform into itself under CP. So, the only way that $\vec{d}_n \propto \vec{s}_n$ and $\vec{d}_n \propto -\vec{s}_n$ can hold true simultaneously is if $|\vec{d}_n| = 0$ exactly. By looking at eq. 24, this means that if $\theta \neq 0$, CP symmetry is violated in QCD, whereas if $\theta = 0$, CP symmetry is preserved. Hence, θ is the parameter that contributes to CP violation in the Strong interaction.

Experiments that test for CP violation in QCD typically measure $|\vec{d}_n|$. This is most simply done using Larmor precession experiments where many spin-up neutrons are placed in an external electromagnetic field, and their precession rates are measured for different configurations of the field directions [7, 20]. In doing so, the strongest experimental constraint on the nEDM magnitude to date is [25]:

$$|\vec{d}_n| < 3 \times 10^{-26}\, e \cdot \text{cm}. \tag{25}$$

This implies that the θ parameter has an upper bound of:

$$|\theta| \lesssim 10^{-9}. \tag{26}$$

There is no reason to expect why the magnitude of θ should be extremely small, so the fact that it is observed to be so small is considered to be a fine-tuning problem in the theory that has been dubbed the "strong CP problem." Therefore, efforts to solve the strong CP problem center on proposing a dynamical way for θ to approach zero.

1.3 Dark Matter

In this subsection, I momentarily switch gears to discuss the nature of dark matter, which helps motivate the introduction to axion physics in Section 2. As early as the 1930s, astrophysicists speculated whether our galaxy contained much more mass than is visible from light emissions from the stars, leading astronomer Fritz Zwicky to coin the term "dark matter" to denote this missing matter. Using more sophisticated measurements of galactic rotation curves in the 1970s (see Fig. 2), Vera Rubin and Kent Ford determined that most galaxies appeared to contain approximately six times matter than is visible from luminosity measurements [26]. This was followed in the 1980s by the development of the Lambda Cold Dark Matter (LCDM) model of cosmology by Jim Peebles and others. The LCDM model provided a theoretical framework for explaining why the existence of cold (non-relativistic) dark matter was necessary for explaining a wide range of cosmological phenomena [27]. I will briefly discuss two of these phenomena below.

First, one of the fundamental tenets of general relativity is that massive astronomical objects such as stars, galaxies, and galaxy clusters distort the spacetime geometry surrounding them. This

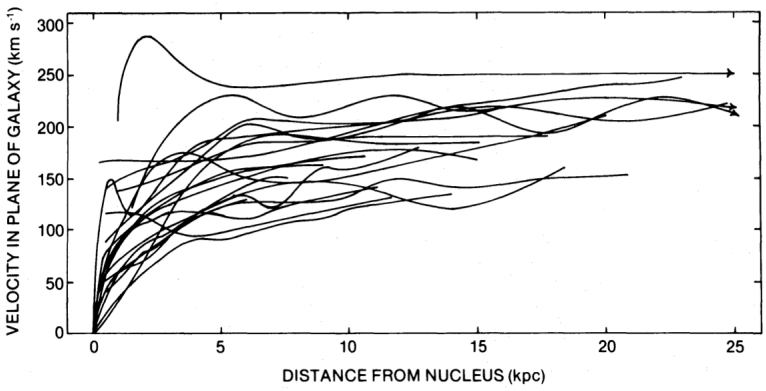

Figure 2: The original galactic rotation curves measured by Rubin [26]. Due to the virial theorem, the flattened velocity distribution at large distances from the galactic center indicates that more mass is present in galaxies than can be visibly observed.

in turn would cause light rays passing by these objects to also be distorted. This effect is known as gravitational lensing. Crucially, by measuring the gravitational lensing effect of light passing by massive objects, physicists can deduce the mass of the object causing the distortion [28]. In doing so for a wide variety of astronomical objects, physicists realized that the amount of distortion was far too great to be caused by the amount of visible matter in those objects. This strongly implied that there was hidden "dark matter" in these objects that contributed to the gravitational effects, but did not interact with ordinary matter via any Standard Model mechanism. Additionally, astronomical observations of the Bullet Galaxy Cluster using gravitational lensing strongly implied that the dark matter in that cluster must be collisionless, i.e. have very weak self-interactions [29].

Second, in the context of cosmological perturbation theory in the LCDM model, it is known that all cosmological structures such as stars and galaxies originated from the growth of matter perturbations in the early Universe [28, 29]. However, such perturbations could only grow linearly with the expansion of the Universe during the period when matter was the dominant form of energy-density in the Universe (from redshift $z = 3500$ to $z = 0.5$). Since baryonic matter could not begin clumping and grow until after it had decoupled from the baryon-photon plasma at redshift $z = 1000$, there is not enough time for the baryonic matter alone to grow to the observed structure sizes today. Therefore, there must exist dark matter that does not couple to photons, so that such DM instabilities could begin clumping from $z = 3500$ and contribute to the deeper gravitational wells needed to explain the observed structure sizes today [29, 30]. Furthermore, this DM must be cold (non-relativistic) during structure formation so that large-scale structures are formed from the bottom-up (i.e. galaxies grouped together to form galaxy clusters), which agrees with astronomical observations [30] (as opposed to the hot, relativistic DM model that leads to top-down structure formation where galaxy clusters form first and then fragment into galaxies).

Measurements made by precision cosmology experiments during the 1990s-2010s, such as COBE, WMAP, and Planck, provided definitive evidence of the veracity of the LCDM model, thereby making LCDM the accepted "Standard Model of Cosmology" [4]. However, despite the abundance of indirect observational evidence for the existence of DM that was discussed above, physicists have yet to directly detect DM or elucidate any information about its particle nature. The sole consensus among cosmologists and particle physicists is that any DM candidate must satisfy the following

three requirements. First, it must be an unknown collisionless particle that either does not interact or interacts extremely weakly with any Standard Model particle. Second, it must have been non-relativistic since the early Universe. Third, it must be stable or long-lived so that even the primordial DM formed during the early Universe still exists today. Despite these requirements, there exists an extremely diverse range of candidates for dark matter particles, spanning roughly 30 orders of magnitude in mass.

One of the leading candidates for the particle nature of DM has been the Weakly Interacting Massive Particles (WIMPs). WIMPs have a mass in the GeV to TeV range, and their predicted properties were obtained as follows: if we assume that the candidate DM particles were thermally created in the early Universe via a similar mechanism as SM particles, then the cross-section of such a DM particle that would lead to the observed DM energy density today would correspond to a new particle with mass similar to the electroweak unification scale at 100 GeV - 1 TeV [19]. In what is known as the WIMP miracle, a particle of exactly this mass was predicted to be the lightest (and thereby most stable) one in the supersymmetry (SUSY) theory [31]. In SUSY, every known fermion in the SM has a "hidden" boson partner, and vice versa [1,3]; this would provide a natural way for eliminating the fine-tuning of the hierarchy problem mentioned at the beginning of Section 1. Despite the attractive nature of SUSY and WIMPs, numerous WIMP search experiments over the years, such as LUX and XENON, have ruled out a large parameter class of WIMPs [32, 33], meaning that more exotic WIMP models may be needed to be viable candidates for DM. This has motivated physicists in recent years to extend their search for DM candidate particles to other types, such as the axion.

2 Introduction to Axion Physics

As I mentioned at the end of Section 1.2, efforts to eliminate the fine-tuning associated with the lack of observed CP violation in the Strong interaction often focus on creating extensions to the Standard Model whereby θ can dynamically fall to a value of zero. In 1977, Roberto Peccei and Helen Quinn proposed a solution to the strong CP problem that did exactly that. In their solution, which is called the Peccei-Quinn theory, they posited the existence of a new, hypothetical pseudoscalar field that dynamically takes θ to zero during the early Universe [34]. Just one year later, in 1978, Frank Wilczek and Steven Weinberg realized that such a quantum field must have an associated particle [35, 36]. Wilczek named this particle the "axion" after a popular brand of detergent at the time, since this hypothetical particle appeared to "clean up" the fine-tuning issue in QCD. In this section, I will discuss how the axion solves the strong CP problem and introduce how its proposed properties make it an attractive candidate for dark matter.

2.1 The Axion Solution to the Strong CP Problem

The Peccei-Quinn theory solves the Strong CP problem by proposing the existence of an additional $U(1)_{PQ}$ global chiral symmetry in the Standard Model, known as the Peccei-Quinn symmetry [7,34]. When this symmetry is spontaneously broken, which occurs at energies below f_a (to be defined below eq. (27)), a dynamical CP-conserving field arises. Due to the nature of the $U(1)_{PQ}$ symmetry, the particle associated with this field is a pseudoscalar, spinless, light, and neutral boson known as the axion. It is precisely this axion field that replaces the static and fine-tuned θ in the old QCD theory. The manner in which the axion field replaces the θ can be seen as follows. The $U(1)_{PQ}$ symmetry introduces an axion field term that couples to the gluon fields in the QCD Lagrangian. When combined with the original θ CP-violating term, the relevant gluon-coupled terms in the

Lagrangian become [7, 19–21]:

$$\mathcal{L} = \left(\frac{a}{f_a} + \theta\right) \frac{g_s^2}{32\pi^2} G_a^{\mu\nu} \tilde{G}_{a\mu\nu}. \tag{27}$$

Here, a refers to the axion field and f_a is the order parameter associated with the breaking of the $U(1)_{PQ}$ symmetry when the axion field is acted on by the symmetry; it is commonly called the Peccei-Quinn symmetry-breaking scale. The $(a/f_a + \theta)$ prefactor in eq. (27) can be treated as the new effective vacuum angle of the theory. From the form of eq. (27), it is apparent that this Lagrangian is invariant under the following $U(1)_{PQ}$ symmetry transformation:

$$a \to a + \alpha f_a; \qquad \theta \to \theta - \alpha. \tag{28}$$

If QCD effects were ignored, then the $U(1)_{PQ}$ symmetry would not restrict the values that the axion field is allowed to take. However, including QCD effects means that the axion field will experience an effective potential that is periodic in the effective vacuum angle [7]:

$$V_{\text{eff}} \sim \cos\left(\frac{a}{f_a} + \theta\right). \tag{29}$$

All scalar fields seek to attain the state where the effective potential that they experience is minimized. Therefore, by taking the derivative of V_{eff} with respect to the field and setting it equal to zero, it is clear that the minimum of the effective potential occurs at $a = -f_a\theta$. This means the axion field will dynamically settle at $a = -f_a\theta$, which is known as its vacuum expectation value. When this value of the axion field is plugged into the modified Lagrangian of eq. (27), it is clear that the axion field will exactly cancel out the CP-violating θ term, thus leaving the QCD Lagrangian invariant under CP. In other words, the presence of the axion "rotates" away the CP-violating angle and eliminates the CP-violating term in the Lagrangian. Hence, the existence of the axion field solves the strong CP problem.

2.2 Cosmological Properties of Axions

Originally, Peccei and Quinn proposed their theory of the axion field solely to create a dynamical way for eliminating the fine-tuning associated with the lack of observed CP violation in the Strong interaction. However, in the early 1980s, Pierre Sikivie and other physicists realized that this very same hypothetical axion could also be a viable dark matter candidate [37, 38]. In this subsection, I will discuss how the theoretical properties of axions make it a viable candidate for comprising at least some, if not all of the dark matter.

First, the existence of axions would have affected the cosmology of the early Universe. During the very early Universe, when its temperature was above f_a, the $U(1)_{PQ}$ symmetry was not broken and the axion field does not exist. However, once the temperature of the Universe dropped below f_a, the PQ phase transition occurred and the $U(1)_{PQ}$ symmetry was spontaneously broken. However, this temperature was still much higher than the QCD phase transition, so the relevant QCD effects that produce the effective potential of the axion field do not manifest themselves yet. Hence, the axion remains massless and the axion field can take any value.

Now, it is necessary to consider when the PQ spontaneous symmetry-breaking occurred in the context of inflation, because this will affect the mechanisms by which axions contribute to the dark

matter energy density [7, 21]. In the first case, if inflation occurred after the PQ symmetry is broken, then the axion field was homogenized by inflation and any topological defects associated with axions were completely diluted away after inflation. In the second case, if inflation occurred before the PQ symmetry is broken, then it would appear to the axions that inflation never occurred, so all topological defects associated with axions remain. These defects include axion strings and domain walls whose decays contribute to the dark matter energy density. For simplicity in this paper, I will henceforth only consider the first case so that a discussion of the more complicated topological structures of axions will not be necessary.

Once the temperature of the early Universe cooled further to the QCD phase transition at 1 GeV, QCD effects manifest themselves and the effective potential given in eq. (29) turns on. At this point, the axion field begins to oscillate about the minimum of V_{eff}. Now, assuming that the axion field was already homogenized by inflation, then the initial amplitude of the oscillation depends on how far from the minimum the axion field was at the QCD phase transition. Furthermore, because the axion is already so light, the axion field oscillations do not dissipate into any other form of energy, and all of the coherent oscillations of the field as it settles at the minimum of V_{eff} contribute to the energy density of the Universe. This contribution is known as the axion misalignment or vacuum realignment mechanism [19, 21].

As the axion field experiences V_{eff} and begins to oscillate about the minimum, the axion gains mass. From our course material, we know that the mass term for a pseudoscalar spinless field should correspond to the second-order term in the Lagrangian. So this gives:

$$m_a^2 \sim \left.\frac{\partial^2 V_{\text{eff}}}{\partial a^2}\right|_{a_{\text{min}}} \sim \frac{1}{f_a^2}. \tag{30}$$

In other words, the mass of the axion should be inversely proportional to f_a. A more exact formula for the axion mass is obtained by considering that axions couple to gluons (to be discussed further in Section 2.4), and in such a coupling, there is a quark-antiquark pair (i.e. meson) involved. Since pions are the lightest meson, axions can readily mix with neutral pions [19]. So on dimensional grounds, the axion mass should have the following dependence:

$$m_a \sim \frac{f_\pi m_{\pi^0}}{f_a} \sim 1\,\mu\text{eV}\left(\frac{10^{13}\,\text{GeV}}{f_a}\right), \tag{31}$$

where $f_\pi = 92$ MeV is the pion decay constant and $m_{\pi^0} = 135$ MeV. Astrophysical and cosmological constraints (to be discussed in Section 2.3) show that f_a is necessarily very large, so that m_a is correspondingly very small. While one might suppose that very light axions would be relativistic during the early Universe (similar to neutrinos), it turns out that the axions produced when the axion field gains mass at the QCD phase transition have momenta on the order of 10^{-8} eV/c [37,39]. This means axions are non-relativistic as soon as they are created.

In addition to having a very light mass, axions also have very weak coupling strengths to SM matter such as photons and electrons, while their own self-interactions are essentially negligible. As I will elaborate further in Section 2.4, in almost all models of axions, they do not couple to photons or electrons at tree level, so all couplings are higher-order, smaller effects. In particular, eq. (37) and eq. (38) show that $g_{a\gamma\gamma}$ and $g_{a\bar{e}e}$ are both inversely proportional to f_a. Since f_a is very large, the axion couplings are very small. Finally, calculation of the axion decay rate using

the higher-order Feynman diagram of the axion-photon coupling (see Fig. 5), which is beyond the scope of our course as it involves a loop diagram, yields the following result for the natural decay time of the axion [21]:

$$\tau_a = \frac{1}{\Gamma_{a\to\gamma\gamma}} = \left(\frac{1\,\text{eV}}{m_a}\right)^5 10^{16}\,\text{years}. \tag{32}$$

So it is clear for any viable axion mass range that axions decay on a time-scale much longer than the age of the Universe. Therefore, since axions do not self-interact (i.e. they are collisionless), weakly couple to SM matter, are long-lived, and are non-relativistic, they constitute a promising candidate for dark matter.

To conclude this subsection on the cosmological properties of axions, I briefly mention the two primary sources of axions in Nature. First, there are the primordial axions that were created during the early Universe via the axion misalignment mechanism described above. They are also commonly known as halo axions because today, they are predominantly found in the gravitational wells formed by the dark matter halos of galaxies and galaxy clusters [37]. Second, there are stellar axions that are produced in stars [21], primarily through the inverse Primakoff process that will be discussed in Section 3.1. It is unsurprising that stars are the other primary source of axions because they contain an abundant number of photons in a strongly magnetic plasma, which can produce axions. As I will discuss in Section 3, one of the two main classes of axion experiments tries to detect either halo or stellar axions.

2.3 Astrophysical and Cosmological Bounds on Axion Mass

Once it was established that axions were a suitable candidate for CDM, physicists sought to place bounds on the allowed mass of the axion so that it could be searched for in laboratory experiments. Such bounds arose from multiple areas of physics: high-energy accelerator physics experiments, astrophysical observations, and cosmological considerations, all of which I discuss below.

First, when Peccei and Quinn first proposed the axion, they believed it was a massive particle with GeV scale mass since it was believed to be similar to the Weak symmetry-scale breaking energy factor. This type of axion was known as the PQWW model axion [19,39]. In principle, such axions could have been detected in Weak-mediated decays of the pi meson:

$$\pi^+ \to a(e^+e^-) + e^+ + \nu_e, \tag{33}$$

where $a(e^+e^-)$ means the hypothetical axion that is produced should rapidly decay into an electron-positron pair. However, high-energy accelerator searches for this process gave negative results for extra electron-positron pairs, thereby ruling out axion models with $m_a > 1$ MeV. Further particle physics constraints were obtained from beam dump experiments where axions are hypothetically produced by many different processes with independent couplings, such as axion-neutral pion mixing and axion coupling to photons, gluons, and quarks. By measuring the cross-sections of such processes, physicists ruled out $m_a \geq 50$ keV [39, 40].

Astrophysical constraints on the axion further reduced its mass range. If axions exist, they should be produced in copious amounts by stars due to the axion-photon and axion-electron coupling that will be discussed in Section 2.4 [41, 42]. Such stellar processes include:

$$\gamma + e \to a + e; \qquad e + N \to N + e + a; \qquad \gamma + N \to N + a, \tag{34}$$

where N denotes a nucleon. The first process is axion-like Compton scattering, the second process is axion bremsstrahlung, and the third process is a form of the Primakoff effect. Notice that axions only appear as products in these processes. This means that emission of axions allows a star to lose energy efficiently because the axions can escape the star without rescattering, whereas photons emitted from a star are scattered numerous times before leaving the star. Thus, the existence of the axion would accelerate stellar evolution and is therefore constrained by astronomical observations of the lifetimes of existing stars. For example, astronomers concluded that the abundance of observed red giant stars rules out the mass range $0.5\,\text{eV} < m_a < 200\,\text{keV}$ [41]. The reason is that above 200 keV, the axion is too heavy to be copiously emitted from the stars, whereas below 0.5 eV it is too weakly coupled for red giants to be a reliable measure anymore. For axions with a large coupling to electrons, the lower bound on the excluded range was extended to 10^{-2} eV since the cooling of the helium core of red giants by axion emission would prevent the onset of helium burning, thereby slowing the red giant evolution [43]. Finally, the range $3 \times 10^{-3}\,\text{eV} < m_a < 2\,\text{eV}$ was excluded by observations of Supernova 1987a [41]. Typically, the collapsed supernova core cools solely by the emission of neutrinos that can be detected on Earth. However, if axions of the above mass range were also emitted from the supernova, the core would also cool from this axion emission and the observed neutrino signal would have been significantly shortened.

As discussed above, whereas an upper bound on the axion mass can be obtained from astrophysical measurements, a crude cosmological lower bound can be obtained from simply enforcing that the axion energy density cannot overclose the universe, since we know from WMAP and Planck measurements that the universe has flat curvature. From QFT calculations beyond the scope of our course, the energy density of axion DM due to the vacuum misalignment mechanism yields the following bound on axion mass [7, 37]:

$$\Omega_a \sim \left(\frac{5\,\mu\text{eV}}{m_a}\right)^{7/6} < 1. \tag{35}$$

Combining all of the bounds from particle physics, astrophysics, and cosmology, the following order-of-magnitude cosmological bound on the axion mass is obtained:

$$10^{-6}\,\text{eV} < m_a < 10^{-3}\,\text{eV}. \tag{36}$$

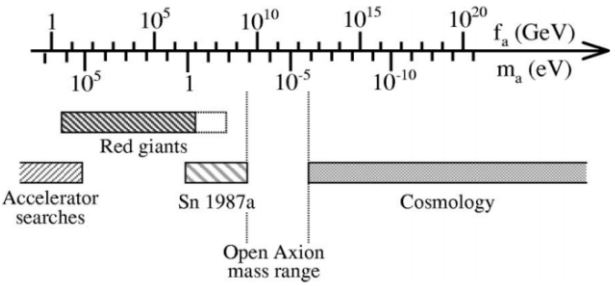

Figure 3: Schematic diagram of the current axion mass range, subject to astrophysical and cosmological constraints. Figure taken from [39].

The corresponding f_a values for this allowed mass range mean that all viable axion models today are known as "invisible axion" models (as opposed to the PQWW "visible axion" model), because they have thus far evaded direct experimental detection.

2.4 Axion Interactions with Standard Model Particles

To conclude this section on the physics of axion dark matter, I discuss how axions interact with Standard Model particles. In particular, knowledge of axion couplings enables experimentalists to design and implement axion detection experiments, which I will discuss in Section 3.

Since axions were created to solve the strong CP problem in QCD, it follows from the CP-violating term in the QCD Lagrangian (eq. (27)) that axions can couple to gluons. However, it turns out that such an axion-gluon coupling does not exist at tree level. Instead, due to QFT reasons beyond the scope of our course, the convention in axion physics is to redefine the quark, axion, and gluon fields in a way that shifts the strength of the axion coupling from the gluons to the quarks (this can be thought of as a "change-of-basis", because gluons and quarks are strongly coupled to each other) [44]. This redefinition of the fields means that in axion physics, the direct axion-gluon coupling vanishes and is replaced by a direct axion-quark coupling. Therefore, the lowest-order axion-gluon coupling comes from a three-vertex loop diagram, as shown in Fig. 4 [19, 44]:

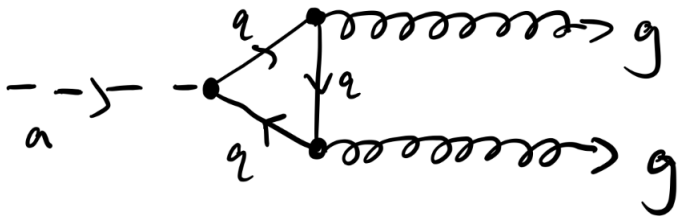

Figure 4: Lowest-order Feynman diagram of the axion-gluon coupling. The convention in axion physics is for axions to couple directly to the quarks via change-of-basis, even though the CP-violating term in the QCD Lagrangian implies that axions directly couple to gluons.

It follows that since quarks participate in QED and the Weak interaction as well, axions can couple to all forms of matter in the Standard Model, albeit always through higher-order processes. To be more precise, there are typically two standard axion models considered by physicists today, which are distinguished by how the axion couples to leptons. In the KSVZ model, axions do not couple to leptons at tree level, meaning that all leptonic couplings come from higher-order diagrams. In the DFSZ model, axions can couple to leptons at tree level [19]. The distinction will be shown in the Feynman diagrams for the axion-electron coupling, to be discussed below.

The two most important axion couplings that I will discuss here, because they are relevant to axion detection experiments, are the axion-photon coupling and axion-electron coupling. In principle, the axion cannot directly couple to photons or electrons because it is electrically neutral and so does not participate in QED. Therefore, axion-photon and axion-electron couplings consist of at least three-vertex loop diagrams at the lowest nonzero order that build upon the axion-quark/gluon coupling mentioned above. This indeed holds true for the KSVZ model axions, although DFSZ models can also exhibit direct axion-electron coupling at tree level.

The axion-photon coupling consists of a single axion that decays into two photons. Because quarks couple to photons in QED, it proceeds through the three-vertex loop diagram shown below in Fig. 5 [44, 45].

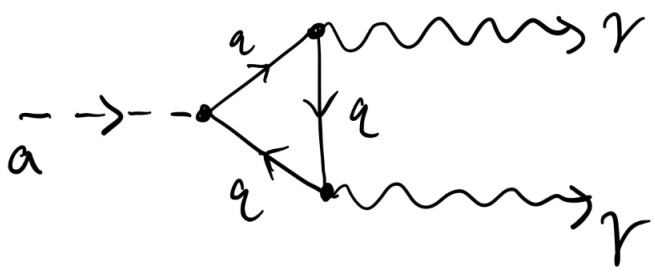

Figure 5: Lowest-order Feynman diagram of the axion-photon coupling.

The Lagrangian associated to this coupling, written in terms of the classical electric and magnetic fields, is [7, 39]:

$$\mathcal{L}_{a\gamma\gamma} = -\left(\frac{\alpha}{2\pi}\frac{C_\gamma}{f_a}\right) a\vec{E}\cdot\vec{B} = -g_{a\gamma\gamma}a\vec{E}\cdot\vec{B}. \tag{37}$$

Here, α is the fine structure constant, while C_γ is a coupling parameter that is model-dependent. For instance, in the KSVZ model, $C_\gamma \sim 0.97$, while in the DFSZ model, $C_\gamma \sim -0.36$. A version of this coupling, known as the Primakoff process, is used in many haloscope/helioscope axion detection experiments, as I will elaborate further in Section 3.

The other coupling of interest is the axion-electron coupling. This coupling is relevant to a new type of axion detection experiment using atomic physics techniques, which I will discuss further in Section 3.3. The coupling consists of an axion that decays into an electron-positron pair. Because quarks and electrons can couple to each other via a virtual photon in QED, the coupling proceeds via the three-vertex bubble diagram shown below in Fig. 6 [19, 44].

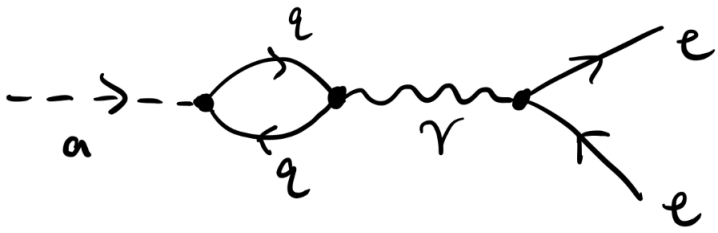

Figure 6: Lowest-order Feynman diagram of the axion-electron coupling. The direct axion-electron coupling, which is a simple tree-level diagram, is not shown here because it is only valid in the DFSZ model.

The Lagrangian associated to the axion-electron coupling is [19, 46]:

$$\mathcal{L}_{a\bar{e}e} = -\left(\frac{C_e m_e}{2\pi f_a}\right)\partial_\mu a\overline{\psi}\gamma^\mu\gamma^5\psi = -g_{a\bar{e}e}\partial_\mu a\overline{\psi}\gamma^\mu\gamma^5\psi, \tag{38}$$

Here, C_e is a coupling parameter that is model-dependent and m_e is the mass of the electron. The insertion of the γ^5 matrix is necessary to enforce the fact that axions are pseudoscalar particles that are odd under parity.

3 Overview of Current Axion Detection Experiments

All axion detection experiments center on the fact that axions can weakly couple to Standard Model particles, in particular the photons and electrons (as discussed in Section 2.4). This means that axion detection experiments actually search for the photons or electrons that axions interact with. Broadly speaking, there are two main classes of axion detection experiments: haloscopes/helioscopes and laser axion experiments. However, in recent years, proposals have been made for a third type of axion detection experiment using atomic/molecular/optical (AMO) physics techniques. In Section 3.3, I will discuss this last technique in detail, including efforts in the DeMille Group at the University of Chicago to explore the implementation of such an axion detection experiment. First, however, I present brief overviews of the other two types of experiments.

3.1 Haloscopes and Helioscopes

The first experimental proposal for direct axion detection was made by Pierre Sikivie in 1983, and takes advantage of the axion-photon coupling shown in Fig. 5 [38]. In particular, the axion-photon coupling can be modified so that one of the emitted photons is treated as a virtual photon due to a static magnetic field (the static field is just a freely propagating photon in the limit of zero frequency). In this case, the axion-photon interaction in the presence of a static magnetic field is known as the Primakoff process. The Feynman diagram for this process is shown below in Fig. 7 [45].

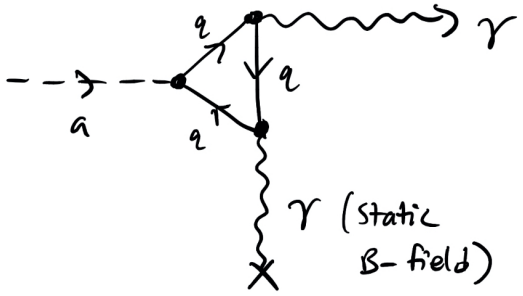

Figure 7: Feynman diagram of the modified axion-photon interaction known as the Primakoff process. The photon ending in an 'x' indicates that it is virtual and due to a static magnetic field.

According to the Primakoff process, axions can resonantly convert to photons in a strong magnetic field. This gave rise to the class of axion detection experiments known as microwave cavity haloscopes. Helioscopes are closely related to haloscopes, except that they detect axions from the Sun. The photons due to solar axions typically have higher energies than cosmic axions and, via the Primakoff effect, are converted to photons in the X-ray frequency range. Therefore, helioscope axion detection techniques differ somewhat from haloscope techniques (i.e. they may only actively point at the Sun during sunrise and sunset) [47]. For brevity in this paper, I will focus the discussion on haloscopes.

Haloscopes aim to detect cosmic axions that are now found in the dark matter halos of every massive and gravitationally bound object in the Universe, including our own galaxy [19]. Because the axions are gravitationally bound to the halo, they must be non-relativistic today. Hence, their

energy can be approximated by:

$$E_a \sim m_a c^2 + \frac{1}{2} m_a c^2 \beta^2, \tag{39}$$

where $\beta \equiv v/c \sim \mathcal{O}(10^{-3})$ due to constraints on the local escape velocity of our galaxy. Since $\beta^2 \sim \mathcal{O}(10^{-6})$, the kinetic energy of cosmic axions can effectively be ignored compared to their rest mass energy. Translating this to a practical experiment, Sikivie suggested that halo axions passing through an electromagnetic cavity permeated with a magnetic field could resonantly convert into photons when the cavity resonant frequency ω matched the axion rest mass m_a [38,39,45]:

$$\hbar\omega = m_a c^2. \tag{40}$$

Using concrete numbers, this means a 5 μeV axion at rest would convert to a 1.2 GHz photon, which can be detected with sensitive microwave receivers. The spread in axion energy due to its kinetic energy would be $\mathcal{O}(10^{-6})$, so a 5 μeV axion would have a 1.2 kHz spread in the frequency of the converted photons. As mentioned in Section 2.3, the axion mass is constrained between approximately 1 μeV and 1 meV, which corresponds to a frequency range for converted photons between 240 MHz and 240 GHz. To maintain the resonant quality of the cavity, however, only a few kHz of bandwidth can be observed at any one time [45]. As a result, the cavity needs to be tunable over a large range of frequencies in order to cover a larger range of values of the axion mass. This is accomplished using metallic or dielectric tuning rods running the length of the cavity cylinder. Moving the tuning rods from the edge to the center of the cavity shifts the resonant frequency by up to 100 MHz [7].

Even when the cavity is exactly tuned to the axion mass, detection is possible only if the microwave receiver is sensitive enough to distinguish the axion conversion signal over the background noise from the cavity and the electronics. With the bandwidth of the experiment essentially set by the axion mass and its kinetic energy dispersion, the signal-to-noise ratio can only be raised by increasing the signal power or integrating for a longer period of time [7,39]. However, both of these actions have limitations. Increasing the signal power comes from either increasing the volume of the cavity or the strength of the magnetic field so that more axions can be converted to photons and be detected, but this is expensive to implement. Integrating over a longer time means that for a given run, there is less time to scan different mass ranges of interest.

The current generation of axion haloscope experiments includes ADMX (Axion Dark Matter Experiment) at the University of Washington [48] and HAYSTAC (Haloscope at Yale Sensitive to Axion Cold Dark Matter) at Yale [49,50]. The latest results from ADMX and HAYSTAC are shown in Fig. 8 below. Note that in axion detection experiments, results are often presented as axion mass versus axion-photon coupling strength. The reason is that both parameters are dependent on each other, since both are inversely proportional to f_a.

3.2 Laser-Induced Axion Experiments

The second main type of axion detection experiments is known as laser-induced axion experiments. Whereas haloscopes and helioscopes detect axions originating from Nature, laser-induced axion experiments take advantage of the axion-photon coupling to detect axions that might be produced from the coherent photons in laser light. The setup of these experiments is typically described as a "light shining through the wall" experiment, as can be seen from the schematic diagram of the experimental setup in Fig. 9.

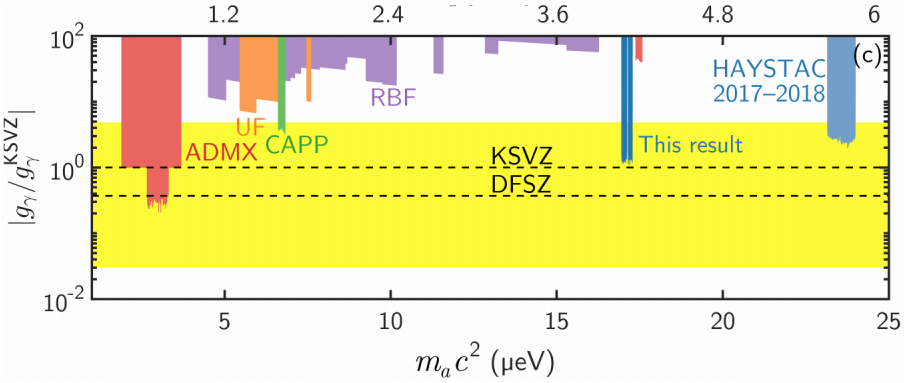

Figure 8: Latest results (2021) from the HAYSTAC experiment [50]. HAYSTAC has ruled out $17\,\mu\text{eV} < m_a < 17.3\,\mu\text{eV}$ and $23\,\mu\text{eV} < m_a < 24\,\mu\text{eV}$, up to the KSVZ model coupling strength. The yellow band indicates the cosmologically relevant region for axion-photon coupling strengths. Also inlaid on the top are exclusion limits from other axion detection experiments such as ADMX (which has ruled out $2.7\,\mu\text{eV} < m_a < 3.3\,\mu\text{eV}$, up to KSVZ model coupling strength).

The operating principle rests on the premise of shining laser light through a region with a strong magnetic field. An optical barrier partitions the magnetic field region into two sections, so that laser light cannot pass from the left section to the right section. However, the photons from the laser light may be stimulated by the external magnetic field in the left section and undergo the inverse Primakoff process to produce axions. These axions will continue to travel in the direction of the laser light momentum and will not be impeded by the optical barrier. Once the axions pass the barrier and enter the right section, they experience a strong magnetic field again. This can induce the axions to undergo the Primakoff process and decay into real photons that can then be detected and analyzed to determine the properties of the axions.

Experiments of this type included the BRFT experiment at Brookhaven National Laboratory in the 1990s [51] and, more recently, the OSQAR experiment at CERN [52]. The most recent result obtained by OSQAR (2014) gave the following bound on the axion-photon coupling, assuming a massless axion: $g_{\alpha\gamma\gamma} < 5.7 \times 10^{-8}\,\text{GeV}^{-1}$.

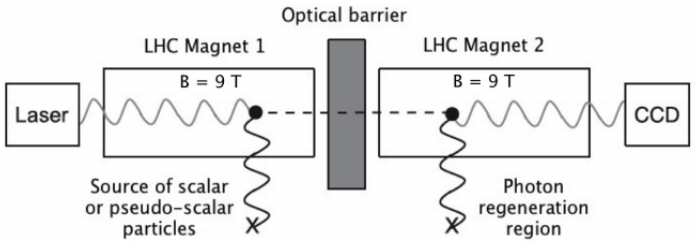

Figure 9: Setup of a typical laser-induced axion experiment. As described in Section 3.2, the magnetic field region is partitioned into two sections so that axions can be produced from the laser light, pass through the partition, and decay back to photons that can then be detected. Figure taken from [52].

3.3 Using AMO Techniques to Detect Axions

Recently, there has been interest in using new experimental platforms to detect axions. In 2014, Pierre Sikivie proposed that techniques from atomic, molecular, and optical (AMO) physics could be used to realize tabletop experiments that could probe the axion mass [46]. In this subsection, I elaborate on the underlying physics of these new AMO tabletop axion detection experiments and discuss the experimental setup and current progress of this new platform.

In contrast to the previous experiments discussed in Section 3.1 and Section 3.2 that utilize the Primakoff effect to detect the photons produced from axion-photon interactions, this new type of experiment uses the axion-electron coupling shown in Fig. 6. The axion interactions with electrons in the AMO system are non-relativistic by nature, so it suffices to work in the non-relativistic limit of the Lagrangian for axion-electron coupling (eq. (38)). This gives the following Hamiltonian for the interaction between an axion and an electron-positron pair [46]:

$$H_{a\bar{e}e} = \frac{g_{ae}}{2f_a}\nabla a \cdot \vec{\sigma}. \tag{41}$$

This Hamiltonian is qualitatively the same as the coupling of the magnetic field to spin, with ∇a playing the role of the magnetic field. Now, from basic quantum mechanics, the ground state of many atoms is related to nearby states by flipping the spin of one or more valence electrons in the atom. Therefore, an excitation of the atom that causes it to go from the ground state to a nearby excited state corresponds to flipping the spin of one or more of the valence electrons.

AMO axion detection experiments utilize this fact of quantum mechanics and the axion-electron coupling in the following manner. When an axion passes by an atom with one valence electron, it can interact with the electron via the axion-electron coupling. In particular, if the axion has the same mass as the transition energy between the ground state and one of the excited states, then the axion-electron interaction will excite the atom to that excited state, which flips the spin of the electron. Once the electron spin is flipped, the atom will eventually decay back to the ground state and emit a photon that can be detected. Assuming the experiment is placed in a low background noise environment to minimize detection of spurious photons, then detection of the photon and analysis of its properties will reveal the mass of the axion that caused the initial spin flip in the atom. It is anticipated that this type of detector will be most sensitive to galactic halo axions that already move at non-relativistic speeds.

Since it is rare for a halo axion passing through a given space to directly encounter an electron and interact with it, AMO axion detection experiments require samples of an extremely large number of atoms, ideally on the order of Avogadro's number, to maximize the number of possible axion detection events. This rules out the use of trapped ultracold atomic gases since the atom number in those platforms is typically only around $\mathcal{O}(10^9)$ atoms. Instead, the most viable platform is rare-earth ions embedded in a solid-state crystal. This platform has the advantage of providing $\mathcal{O}(10^{23})$ atoms fixed in space. Furthermore, the techniques used to probe such systems are well-known, having been used in other fields such as quantum information. It turns out that for a mole of target atoms, the transition rate to the excited state due to axions causing a spin flip is [46, 53]:

$$N_A R_i = g_i^2 N_A \overline{v^2} \frac{2\rho_a}{f_a^2} \min(t, t_1, t_a). \tag{42}$$

Here, N_A is Avogadro's number; R_i is the transition rate to the ith excited state; g_i is an $\mathcal{O}(1)$ parameter giving the coupling strength of the target atom; $\overline{v^2}$ is the average squared velocity of the

halo axion; ρ_a is the cosmic axion energy density; t, t_1, and t_a are experimental parameters relating to measurement time, lifetime of the excited state, and coherence time of the signal, respectively. It is clear from eq. (42) that t, t_1, and t_a are the most important parameters to optimize in order to obtain a good signal. Based on this, Sikivie determined the proposed sensitivity of such a detector to the axion-electron coupling and axion mass, which is shown in Fig. 10. In particular, the AMO axion detector is predicted to be sensitive to nearly the entire viable axion mass range of $10^{-6}\,\text{eV} < m_a < 10^{-3}\,\text{eV}$, which is a substantial improvement over current haloscope experiments.

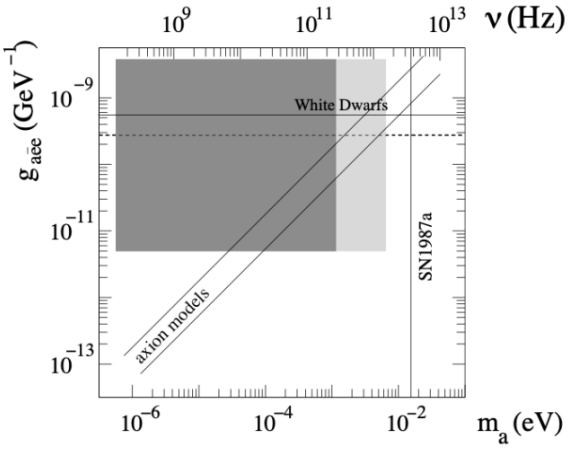

Figure 10: Proposed sensitivity of the AMO axion detector to the axion-electron coupling and axion mass. Dark gray indicates the detector-sensitive region, with reference limit lines from astrophysical sources (white dwarfs and Supernova 1987a). The diagonal lines indicate the mass-coupling degeneracy line of predicted axion models such as KSVZ and DFSZ. Figure taken from [46].

In 2017, an Italian group [53] realized a proof-of-principle experimental scheme based on Sikivie's proposal. They chose a $YLiF_4$ crystal doped with Er^{3+} ions (Er:YLF). A diagram of their scheme is shown in Fig. 11. In their setup, the ground state of their ions is Zeeman split using an external tunable magnetic field. The lower state corresponds to the original ground state and the excited state corresponds to the spin-flipped state. To probe the relevant axion mass range, the B-field is split to approximately 1 meV. As discussed earlier, if a halo axion of mass $m_a \sim 1$ meV passes by and excites the ion, it flips the spin up to the excited state. Then, a pump laser with high power is sent through the crystal. It will excite those spin-flipped ion to a much higher energy level, whereby when the ion decays from that energy level, it emits visible or near-infrared (NIR) photons that can be readily detected using photodiodes or photomultiplier tubes. Crucially, the crystal of ions must be cooled to mK temperatures using liquid helium in order to prevent false positive detections where the atom could be thermally excited from the ground state to the excited state. This temperature is roughly given in terms of the f_a scale as [53]:

$$T = 12\,\text{mK}\left(\frac{10^{11}\,\text{GeV}}{f_a}\right). \tag{43}$$

While the Italian group has not obtained concrete limits on the axion mass or axion-electron coupling yet, they did determine the values of many of the experimental parameters necessary for realizing such a tabletop AMO scheme for detecting axions [53].

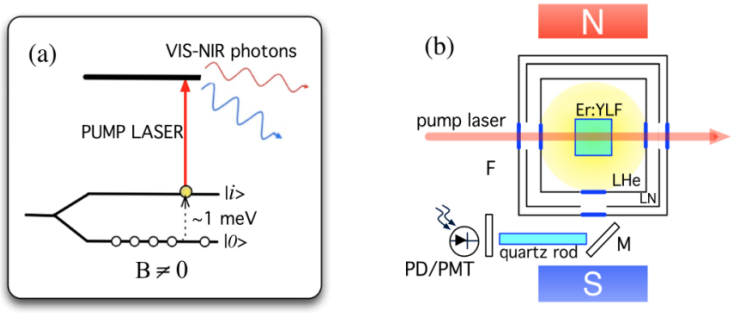

Figure 11: Schematic of the Italian group's AMO axion detector experimental setup. (a) shows the level structure of the ions in the Er:YLF crystal; $|0\rangle$ denotes the ground state and $|i\rangle$ denotes the Zeeman-split excited state that the axion can excite the ion to. (b) shows the rough setup of the experiment. Note that the Er:YLF crystal is placed in liquid He to reduce thermal noise, and the external magnet (N, S) is used to provide the Zeeman splitting. Figure taken from [53].

To conclude, I will briefly mention a competing implementation of Sikivie's AMO axion detection experiment proposal that is in the exploratory stages here in the DeMille Group at the University of Chicago. In our group's implementation, we plan to use Thulium ions doped in a Calcium Fluoride crystal (Tm^{2+}:CaF_2) as the platform for our experiment. When doped in the crystal, these ions have one hole in their outermost 4f shell, which means they effectively behave as spin-1/2 particles with one valence hole instead of one valence electron [54]. Using the standard formula for Zeeman splitting of the ground state, an external magnetic field of 1-10 T is needed to split the absolute ground state of this system to be sensitive to axion masses in the range 0.1-1 meV. Once an axion passes through the crystal and flips the spin of one of our ions, we will use an 1115 nm NIR laser to drive the spin-flipped atoms from the $^2F_{7/2}$ ground state to the $^2F_{5/2}$ excited state. This transition wavelength was determined from known spectroscopy measurements of the Tm^{2+}:CaF_2 crystal [55]. Similar spectroscopy measurements also show that the lifetime of the spin-flipped state is approximately 1 ms [56]. From the $^2F_{5/2}$ excited state, we will induce another optical transition up to the 5d valence band states, this time using a broadband NIR laser. The 5d band states have extremely short lifetimes on the order of 100 ns [55], and when they decay, they emit visible photons that can then be detected. Therefore, by pulsing on our 1115 nm laser every 1 ms, we can ensure that any ions in our system that have had their spin flipped by a halo axion will transition up to the 5d band and emit a photon. Subsequently, we can use photon-detection and counting techniques to determine whether any cosmic axions have passed through our system. A schematic figure of what I have described is shown in Fig. 12.

4 Summary and Conclusion

In this final paper, I have endeavored to provide a comprehensive introduction to the rich topic of axion physics. Below, I summarize the main points of what I have discussed throughout the paper.

In Section 1, I introduced the particle physics motivations for the existence of the hypothetical axion particle. Although particle physicists had long believed that discrete symmetries were fundamental symmetries of Nature, experimentalists in the 1950s and 1960s discovered that parity and charge conjugation-parity symmetry were violated in the Weak interaction. After this fact

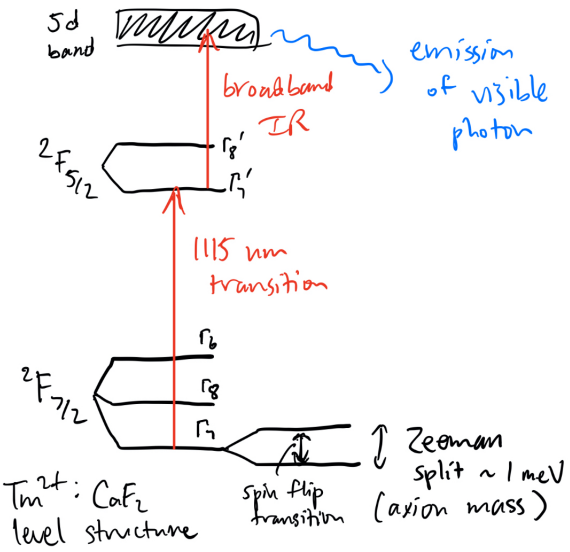

Figure 12: Ionic level structure of the Tm^{2+}:CaF_2 solid-state crystal system that is proposed to be used as an axion detector in the DeMille group. The Zeeman splitting allows for hypothetical cosmic axions of the appropriate mass to cause a spin flip. Once flipped, lasers will drive the ions to higher excited states, where they will decay and emit visible photons that will be detected to deduce properties of the axion.

was incorporated into the Standard Model, physicists soon realized that the strong interaction should theoretically also exhibit CP violation. However, CP violation has never been experimentally observed in strong interaction-mediated processes, leading to a fine-tuning problem with the Standard Model known as the strong CP problem. Simultaneously, on a seemingly unrelated front, cosmological evidence of the existence of dark matter led particle physicists to search for candidate particles that could elucidate the particle nature of dark matter.

In Section 2, I introduced the basic principles of axion physics. Peccei, Quinn, Weinberg, and Wilczek hypothesized the existence of an extremely light, pseudoscalar, spinless boson field known as the axion that could dynamically make the CP-violating term in the QCD Lagrangian very small, thereby solving the strong CP problem. Shortly thereafter, Sikivie and others realized that this same axion had all of the right properties to be an attractive candidate for dark matter. This motivated physicists to commence searching for axions. Using high-energy accelerator searches and astrophysical/cosmological bounds, physicists were able to narrow the mass range of axions to roughly $10^{-6}\,\text{eV} < m_a < 10^{-3}\,\text{eV}$. This led physicists to dub the surviving axion models as "invisible axions" because their extremely light mass has enabled them to evade direct detection thus far. However, because of their weak couplings to Standard Model particles, in particular photons and electrons, experimentalists have devised ingenious methods for detecting these "invisible axions."

In Section 3, I introduced the main types of axion detection experiments today. These experiments can roughly be divided into two classes: haloscopes/helioscopes and laser-induced axion experiments. The haloscope experiment was first proposed by Sikivie in the 1980s to search for cosmic axions in the dark matter halo of our galaxy, and is based on the fact that because axions can couple to photons, they can also resonantly convert to photons in the presence of a strong

magnetic field. Detection of the photons then allows physicists to deduce properties of the axion. Laser-induced axion experiments are also based on the axion-photon coupling, though they search for axions produced from artificial laser light. Finally, I concluded the section by introducing a new type of axion detection experiment that is still in the exploratory stages. This new experiment will use AMO techniques to search for axions and is based on the axion-electron coupling instead of the axion-photon coupling.

To conclude, axion physics is an extremely rich and fascinating topic in modern particle physics research. If axions are detected in the future, they would simultaneously solve two of the most outstanding problems in the Standard Model: the strong CP problem and the particle nature of dark matter. With ever-improving technologies and new experimental efforts in axion detection, the future for axion physics looks extremely bright and promising!

References

[1] David Griffiths. *Introduction to Elementary Particles*. John Wiley & Sons, 2nd revised edition, 2020.

[2] Mark Thomson. *Modern Particle Physics*. Cambridge University Press, 2013.

[3] John Ellis. Outstanding Questions: Physics Beyond the Standard Model. *Philosophical Transactions of the Royal Society A: Mathematical, Physical and Engineering Sciences*, 370(1961):818–830, 2012.

[4] N Aghanim et al. Planck 2018 Results. VI. Cosmological Parameters. *arXiv preprint arXiv:1807.06209*, 2018.

[5] Andrei D Sakharov. Violation of CP-invariance, C-asymmetry, and Baryon Asymmetry of the Universe. In *In The Intermissions... Collected Works on Research into the Essentials of Theoretical Physics in Russian Federal Nuclear Center, Arzamas-16*, pages 84–87. World Scientific, 1998.

[6] Nima Arkani-Hamed, Savas Dimopoulos, and Gia Dvali. The Hierarchy Problem and New Dimensions at a Millimeter. *Physics Letters B*, 429(3-4):263–272, 1998.

[7] Markus Kuster, Georg Raffelt, and Berta Beltrán. *Axions: Theory, Cosmology, and Experimental Searches*. Springer, 2007.

[8] I.I. Bigi and A.I. Sanda. *CP Violation*. Cambridge University Press, 2000.

[9] J. J. Sakurai and Jim Napolitano. *Modern Quantum Mechanics*. Cambridge University Press, 2nd edition, 2017.

[10] Chien-Shiung Wu. The Discovery of the Parity Violation in Weak Interactions and its Recent Developments. In *Nishina Memorial Lectures*, pages 43–70. Springer, 2008.

[11] T. D. Lee and C. N. Yang. Question of Parity Conservation in Weak Interactions. *Phys. Rev.*, 104:254–258, Oct 1956.

[12] C. S. Wu, E. Ambler, R. W. Hayward, D. D. Hoppes, and R. P. Hudson. Experimental Test of Parity Conservation in Beta Decay. *Phys. Rev.*, 105:1413–1415, Feb 1957.

[13] Lev Landau. On the Conservation Laws for Weak Interactions. *Nuclear Physics*, 3(1):127–131, 1957.

[14] J. H. Christenson, J. W. Cronin, V. L. Fitch, and R. Turlay. Evidence for the 2π Decay of the K_2^0 Meson. *Phys. Rev. Lett.*, 13:138–140, Jul 1964.

[15] Ashton B. Carter and A. I. Sanda. CP Violation in B-meson Decays. *Phys. Rev. D*, 23:1567–1579, Apr 1981.

[16] Bernard Aubert et al. Observation of Direct CP Violation in $B^0 \to K^+\pi^-$ Decays. *Phys. Rev. Lett.*, 93:131801, 2004.

[17] Q Retal Ahmad et al. Direct Evidence for Neutrino Flavor Transformation from Neutral-Current Interactions in the Sudbury Neutrino Observatory. *Physical Review Letters*, 89(1):011301, 2002.

[18] Y Fukuda et al. Evidence for Oscillation of Atmospheric Neutrinos. *Physical Review Letters*, 81(8):1562, 1998.

[19] Antonios Gardikiotis. *Search for Axions via Astrophysical Observations.* PhD thesis, Patras U., July 2015.

[20] Anson Hook. TASI Lectures on the Strong CP Problem and Axions. *arXiv preprint arXiv:1812.02669*, 2018.

[21] Albert Renau Cerrillo. *Some Theoretical and Experimental Aspects of Axion Physics.* PhD thesis, Universitat de Barcelona, 2015.

[22] Luca Di Luzio, Maurizio Giannotti, Enrico Nardi, and Luca Visinelli. The Landscape of QCD Axion Models. *Physics Reports*, 2020.

[23] Steven Weinberg. The U(1) Problem. *Phys. Rev. D*, 11:3583–3593, Jun 1975.

[24] G. 't Hooft. Computation of the Quantum Effects Due to a Four-dimensional Pseudoparticle. *Phys. Rev. D*, 14:3432–3450, Dec 1976.

[25] C. Abel et al. Measurement of the Permanent Electric Dipole Moment of the Neutron. *Phys. Rev. Lett.*, 124:081803, Feb 2020.

[26] V. C. Rubin, N. Thonnard, and W. K. Ford, Jr. Rotational Properties of 21 SC Galaxies with a Large Range of Luminosities and Radii, from NGC 4605 (R = 4kpc) to UGC 2885 (R = 122 kpc). *Astrophys. J.*, 238:471, 1980.

[27] P. J. E. Peebles. Tests of Cosmological Models Constrained by Inflation. *Astrophys. J.*, 284:439–444, 1984.

[28] Scott Dodelson and Fabian Schmidt. *Modern Cosmology.* Academic Press, 2020.

[29] Mariangela Lisanti. Lectures on Dark Matter Physics. In *Theoretical Advanced Study Institute in Elementary Particle Physics: New Frontiers in Fields and Strings*, 3 2016.

[30] Daniel Baumann. TASI Lectures on Primordial Cosmology. *arXiv preprint arXiv:1807.03098*, 2018.

[31] Gerard Jungman, Marc Kamionkowski, and Kim Griest. Supersymmetric Dark Matter. *Physics Reports*, 267(5-6):195–373, 1996.

[32] DS Akerib et al. Limits on Spin-Dependent WIMP-Nucleon Cross Section Obtained from the Complete LUX Exposure. *Physical Review Letters*, 118(25):251302, 2017.

[33] E. Aprile et al. Dark Matter Search Results from a One Ton-Year Exposure of XENON1T. *Phys. Rev. Lett.*, 121:111302, Sep 2018.

[34] R. D. Peccei and Helen R. Quinn. CP Conservation in the Presence of Pseudoparticles. *Phys. Rev. Lett.*, 38:1440–1443, Jun 1977.

[35] F. Wilczek. Problem of Strong P and T Invariance in the Presence of Instantons. *Phys. Rev. Lett.*, 40:279–282, Jan 1978.

[36] Steven Weinberg. A New Light Boson? *Phys. Rev. Lett.*, 40:223–226, Jan 1978.

[37] J. Ipser and P. Sikivie. Can Galactic Halos Be Made of Axions? *Phys. Rev. Lett.*, 50:925–927, Mar 1983.

[38] P. Sikivie. Experimental Tests of the "Invisible" Axion. *Phys. Rev. Lett.*, 51:1415–1417, Oct 1983.

[39] R. Bradley, J. Clarke, D. Kinion, L. J. Rosenberg, K. van Bibber, S. Matsuki, M. Muck, and P. Sikivie. Microwave Cavity Searches for Dark-Matter Axions. *Rev. Mod. Phys.*, 75:777–817, 2003.

[40] Particle Data Group et al. Review of Particle Physics. *The European Physical Journal C-Particles and Fields*, 3(1-4):1–783, 1998.

[41] Georg G. Raffelt. Astrophysical Axion Bounds. *Lect. Notes Phys.*, 741:51–71, 2008.

[42] Michael S. Turner. Windows on the Axion. *Phys. Rept.*, 197:67–97, 1990.

[43] David S. P. Dearborn, David N. Schramm, and Gary Steigman. Astrophysical Constraints on the Couplings of Axions, Majorons, and Familons. *Phys. Rev. Lett.*, 56:26–29, Jan 1986.

[44] Jihn E. Kim and Gianpaolo Carosi. Axions and the Strong CP Problem. *Rev. Mod. Phys.*, 82:557–601, Mar 2010.

[45] Ian P Stern, ADMX, and ADMX-HF collaborations. Axion Dark Matter Searches. In *AIP Conference Proceedings*, volume 1604, pages 456–461. American Institute of Physics, 2014.

[46] P. Sikivie. Axion Dark Matter Detection Using Atomic Transitions. *Phys. Rev. Lett.*, 113:201301, Nov 2014.

[47] V Anastassopoulos et al. New CAST Limit on the Axion–Photon Interaction. *Nature Physics*, 13(6):584, 2017.

[48] T. Braine et al. Extended Search for the Invisible Axion with the Axion Dark Matter Experiment. *Phys. Rev. Lett.*, 124:101303, Mar 2020.

[49] Alex Droster and Karl van Bibber. HAYSTAC Status, Results, and Plans. In *13th Conference on the Intersections of Particle and Nuclear Physics*, 1 2019.

[50] KM Backes et al. A Quantum Enhanced Search for Dark Matter Axions. *Nature*, 590(7845):238–242, 2021.

[51] R. Cameron, G. Cantatore, A. C. Melissinos, G. Ruoso, Y. Semertzidis, H. J. Halama, D. M. Lazarus, A. G. Prodell, F. Nezrick, C. Rizzo, and E. Zavattini. Search for Nearly Massless, Weakly Coupled Particles by Optical Techniques. *Phys. Rev. D*, 47:3707–3725, May 1993.

[52] Rafik Ballou et al. Latest Results of the OSQAR Photon Regeneration Experiment for Axion-Like Particle Search. In *10th Patras Workshop on Axions, WIMPs and WISPs*, 10 2014.

[53] Caterina Braggio et al. Axion Dark Matter Detection by Laser Induced Fluorescence in Rare-Earth Doped Materials. *Sci. Rep.*, 7(1):15168, 2017.

[54] Zoltan J. Kiss. Energy Levels of Divalent Thulium in CaF_2. *Phys. Rev.*, 127:718–724, Aug 1962.

[55] Judith Grimm, OS Wenger, KW Krämer, and Hans-Ulrich Güdel. 4f–4f and 4f–5d Excited States and Luminescence Properties of Tm^{2+}-doped CaF_2, $CaCl_2$, $SrCl_2$ and $BaCl_2$. *Journal of luminescence*, 126(2):590–596, 2007.

[56] E. S. Sabisky and C. H. Anderson. Spin-Lattice Relaxation of Tm^{2+} in CaF_2, SrF_2, and BaF_2. *Phys. Rev. B*, 1:2028–2040, Mar 1970.